



## Ni-MORDENITE SYSTEM: INFLUENCE OF $\text{SiO}_2/\text{Al}_2\text{O}_3$ MOLAR RATIO ON THE CATALYTIC ACTIVITY IN NO REDUCTION

## SISTEMA Ni-MORDENITA: INFLUENCIA DE LA RELACIÓN MOLAR $\text{SiO}_2/\text{Al}_2\text{O}_3$ EN LA ACTIVIDAD CATALÍTICA PARA LA REDUCCIÓN DE NO

R. Obeso-Estrella<sup>1</sup>, A. Simakov<sup>2</sup>, M. Avalos-Borja<sup>2,3</sup>, F. Castellón<sup>2</sup>, E. Lugo<sup>4</sup> and V. Petranovskii<sup>2\*</sup>

<sup>1</sup>Posgrado en Ciencia e Ingeniería de Materiales, Universidad Nacional Autónoma de México, Centro de Nanociencias y Nanotecnología (PCeIM, CNyN-UNAM), Apdo. Postal 14, C.P. 22800, Ensenada, B.C., México. .

<sup>2</sup>Universidad Nacional Autónoma de México, Centro de Nanociencias y Nanotecnología, Departamento de Nanocatálisis, Apdo. Postal 14, C.P. 22800, Ensenada, B.C., México.

<sup>3</sup>On leave at IPICYT, San Luis Potosí, S.L.P., México.

<sup>4</sup>Departamento de Ingeniería Química, Instituto Tecnológico de Los Mochis, Blvd. Juan de Dios Bátiz y 20 de Noviembre, 81250 Los Mochis, Sinaloa, México.

Received 20 of February 2012; Accepted 31 of October 2012

### Resumen

Se intercambió con  $\text{Ni}^{2+}$  una serie de mordenitas con la relación molar (RM)  $\text{SiO}_2/\text{Al}_2\text{O}_3$  de 13, 20 y 90. Las muestras se caracterizaron por DRX, EDE, ERD y MET. Los espectros de UV-Vis de todas las muestras son típicos para iones coordinados octaédricamente con moléculas de agua de  $\text{Ni}(\text{H}_2\text{O})_6^{2+}$ . En el rango de UV, las muestras con RM de 20 y 90 mostraron la absorción a 250-300 nm efecto de la deshidratación parcial de iones  $\text{Ni}^{2+}$  y su coordinación con  $\text{O}^{2-}$  de la matriz zeolítica. Se reveló que las especies de Ni formadas en la muestra etiquetada como NiNaMor13 con la RM baja están débilmente ligadas a la estructura de mordenita; como una consecuencia se observa una alta actividad catalítica en la reducción de NO. La transformación sencilla de la reducción-oxidación de tales especies causa la activación de la pirólisis de propeno con la formación de nanoestructuras de carbono.

**Palabras clave:** Ni-mordenita, relación molar  $\text{SiO}_2/\text{Al}_2\text{O}_3$ , nanotubos de carbón, reducción de NO, UV-Vis.

### Abstract

Mordenites with  $\text{SiO}_2/\text{Al}_2\text{O}_3$  molar ratio (MR) of 13, 20 and 90 were exchanged with a  $\text{Ni}^{2+}$ . The samples were characterized by XRD, EDS, DRS and TEM. UV-Vis spectra of all Ni-exchanged samples were typical for a  $\text{Ni}(\text{H}_2\text{O})_6^{2+}$  ions octahedrally coordinated by water molecules. In the UV range, samples with MR of 20 and 90 showed absorption around 250-300 nm due to partial dehydration on  $\text{Ni}^{2+}$  ions and their coordination with  $\text{O}^{2-}$  of the zeolite framework. It was revealed that Ni species formed on mordenite NiNaMor13 with low molar ratio are weakly bound to the mordenite framework; as a consequence, high catalytic activity in NO reduction is observed. Easy red-ox transformation of such a species results in the activation of propene pyrolysis with formation of carbon nanostructures.

**Keywords:** Ni-mordenite,  $\text{SiO}_2/\text{Al}_2\text{O}_3$  molar ratio, carbon nanotubes, NO reduction, UV-Vis.

## 1 Introduction

Selective catalytic reduction (SCR) of NO by hydrocarbons is one of the most powerful methods for

the effective control of NO emission Hu *et al.*, (2009), Johnson (2009). Between other materials, metal-modified zeolites are extensively studied as catalysts

\*Corresponding author. E-mail: vitalii@cnyn.unam.mx  
Tel. 01 (646) 174-46-02, ext. 361, Fax 01 (646) 174-46-03

for this process Rebrov *et al.* (1999), Rebrov *et al.* (2000), Yahiro and Iwamoto (2001). The metals most frequently used for zeolite modification are Co, Fe, and Cu Parvulescu *et al.* (1998). Zeolites exchanged with Ni are less studied in this reaction.

There are the different methods of metal incorporation into zeolite frameworks, such as traditional wet impregnation or more complicated ion exchange techniques Martinez and Corma (2011). It is known that the highest content of metals was achieved by solid state ion exchange of protonic zeolites with metal chloride precursors Sazonova *et al.* (1997), Abu-Zied *et al.* (2008).

There are more than 200 zeolite types with different structure of channels and cavities Baerlocher *et al.* (2007). The most applicable zeolites for SCR of NO are ZSM-5, Y, Beta, and Mordenite. It was shown that the SiO<sub>2</sub>/Al<sub>2</sub>O<sub>3</sub> molar ratio (MR) is one of the important parameters managing acidity, ion-exchange capacity, and metal coordination in zeolites Bogdanchikova (1999), Bogdanchikova (2000), Gurin (2002), Gurin (2005).

The aim of the present work was to study influence of MR on the formation of different Ni species in mordenite, and evaluation of their catalytic activity in SCR of NO in the presence of propene and CO.

## 2 Experimental

### 2.1 Catalyst preparation

Mordenites with SiO<sub>2</sub>/Al<sub>2</sub>O<sub>3</sub> molar ratio of 13, 20 and 90 in sodium, ammonium and proton forms, respectively, were supplied by Zeolite International. Ni was incorporated by liquid phase ion exchange of zeolites using an aqueous solution of Ni(NO<sub>3</sub>)<sub>2</sub> at 60 °C under continuous stirring for 24 h. Subsequently, the zeolites were washed thoroughly with deionized water and dried at 110 °C overnight. Through the text and figures samples are denoted as “Ni” if materials were exchanged, followed by exchangeable cations (Na, NH<sub>4</sub>, H) and “Mor” for mordenite, finished with value of SiO<sub>2</sub>/Al<sub>2</sub>O<sub>3</sub> molar ratio; for example NiNaMor13.

### 2.2 Catalyst characterization

The crystallinity of samples before and after ion exchange was tested by XRD measurements using Philips X'Pert diffractometer with Cu K<sub>α</sub> radiation. To

evaluate electronic state of Ni species UV-Vis diffuse reflectance spectra were recorded by a Varian Cary 300 spectrophotometer equipped with an integrated sphere assembly. The spectra were recorded at room temperature using Teflon (HALON) as reference and plotted in terms of absorption. In order to show clearly a presence of nickel species, the spectra of Ni exchanged zeolites presented below were obtained by subtraction of spectrum of corresponding zeolite. The nickel content was measured by energy dispersive spectroscopy (EDS) on a JEOL 5300 Scanning Electron Microscope.

The catalytic activity of the samples in NO reduction in the presence of CO, propene and oxygen was studied in a continuous flow reactor with fixed bed of a catalyst. The mixture (NO-0.09 vol%, C<sub>3</sub>H<sub>6</sub> - 0.22 vol.%, CO - 1.18 vol.%, O<sub>2</sub> - 0.46 vol.%, N<sub>2</sub> - balance) flow was 55 mL/min. 0.1 g of catalyst as a fine powder was supported on quartz wool. The activity characterized by light-off curves of NO conversion vs temperature was measured within 30-550°C temperature interval with a heating ramp of 1 °C/min. Before contact with the reaction mixture samples were pretreated in situ in oxygen within 25-500°C temperature range with a ramp rate of 10 °C/min. NO and NO<sub>2</sub> content was monitored by means of AO2000 gas analyzer.

The high resolution transmission electron microscopy (HRTEM) images of the samples after the catalytic tests were carried out in a FEI Tecnai F30 transmission electron microscope.

## 3 Results and discussion

The chemical composition of the samples is presented in the Table 1. Ni content obtained experimentally was compared with theoretical exchange capacity of the mordenite samples, taking into account their MR value. It means, that as each atom of Al isomorphously substituting Si atom in zeolite framework generate one negatively charged tetrahedra, which have to be equilibrated by positively charged ion. Starting zeolites materials studied in this paper were equilibrated by sodium, ammonium and proton cations. In addition, applied zeolites are characterized with different SiO<sub>2</sub>/Al<sub>2</sub>O<sub>3</sub> molar ratio, that is, with different amount of cations to be exchanged. Therefore, amounts of Ni<sup>2+</sup> substituted cations in elementary cells of Mor13, Mor20, and Mor90 has to be different.

Table 1. Chemical composition and percentage of Ni exchange in the prepared Ni-mordenite samples.

Sample	SiO <sub>2</sub> /Al <sub>2</sub> O <sub>3</sub> <sup>a</sup>	Ni/Al <sup>a</sup> (wt.%)	Ni loading <sup>a</sup>	Theoretic formula for 100% Ni exchange	Estimated formula <sup>a</sup>	Ni exchange (%) degree <sup>b</sup>
NiNaMOR	13	0.3	1.87	Ni <sub>3.2</sub> Al <sub>6.4</sub> Si <sub>41.6</sub> O <sub>96</sub>	Ni <sub>0.6</sub> Na <sub>5.2</sub> Al <sub>6.4</sub> Si <sub>41.6</sub> O <sub>96</sub>	18.8
NiNH <sub>4</sub> MOR	20	0.21	0.9	Ni <sub>2.2</sub> Al <sub>4.4</sub> Si <sub>43.6</sub> O <sub>96</sub>	Ni <sub>0.29</sub> (NH <sub>4</sub> ) <sub>3.8</sub> Al <sub>4.4</sub> Si <sub>43.6</sub> O <sub>96</sub>	13.2
NiHMOR	90	0.44	0.44	Ni <sub>0.5</sub> AlSi <sub>47</sub> O <sub>96</sub>	Ni <sub>0.14</sub> H <sub>0.8</sub> AlSi <sub>47</sub> O <sub>96</sub>	28

<sup>a</sup>From EDS data

<sup>b</sup>Percentage of Ni exchange was estimated as a ratio of observed Ni content and theoretical value of accessible exchange sites, taking into account that each Ni<sup>2+</sup> cation can exchange 2 Na<sup>+</sup> cations.

Indeed, NiNaMor13 is characterized with higher content of Ni than two other samples (NiNH<sub>4</sub>Mor20 and NiHMor90). Therefore, increasing of MR decreases the amount of exchanged Ni. The variation of percent of Ni exchange degree and the lowest observed value for NiMor20 probably is due to difference in cation selectivity for Ni<sup>2+</sup> → Na<sup>+</sup>, Ni<sup>2+</sup> → NH<sub>4</sub><sup>+</sup> and Ni<sup>2+</sup> → H<sup>+</sup> equilibria, complicated by MR dependence. But detailed study of thermodynamic of ion exchange of nickel as a function of exchangeable cations and molar ratio in this set of samples is out of scope of present work.

XRD analysis of catalysts was carried out to confirm stability of the zeolites in initial, exchanged, and spent materials. All samples before and after treatments showed patterns typical for mordenite structure. As an example, Fig. 1 shows the diffraction patterns of starting NaMor13 and exchanged NiNaMor13 samples. No change in the structure and crystallinity of samples was observed after ion exchange. Therefore, one can conclude that no distortion of the mordenite structure during exchange treatment at slightly elevated temperature was observed.

In the UV-Vis spectra of dried Ni-exchanged samples a band at 390-400 nm and a doublet with a maxima at 650 and 720 nm were observed (see Fig. 2), those are representative for Ni<sup>2+</sup> ions in an octahedral oxygen environment, typically Ni(H<sub>2</sub>O)<sub>6</sub><sup>2+</sup> due to a transition A<sub>2g</sub> → T<sub>1g</sub> Lever (1984). Also, spectra of NiNH<sub>4</sub>Mor20 and NiHMor90 showed absorption around 250-300 nm that can be due to partial dehydration on Ni<sup>2+</sup> ions and their coordination with O<sup>2-</sup> of zeolite framework, forming in this way the electron donor-acceptor complex. Therefore, a band of charge-transfer complex can be expected in this region Lever (1984). In contrast, the NiNaMor13 sample shows no absorbance in the ultraviolet region (λ ~

200-350 nm) unlike the other two samples. From this observation, one can deduce that in NiNH<sub>4</sub>Mor20 and NiHMor90 samples nickel species are more strongly linked to the zeolite lattice, in contrary to those in NiNaMor13.

The curves of NO conversion on prepared catalysts are presented in the Fig. 3. NiHMor90 sample shows low activity within studied temperature interval. The value of NO conversion does not exceed 3%.

Catalytic activity of other two samples up to the temperature of 350 oC is also low and comparable to each other. However, further temperature increase leads to drastic increment of catalytic activity only for NiNaMor13 sample up to 100%. The catalytic activity for NiNH<sub>4</sub>Mor20 sample with increasing of temperature first drops down and then increased, but only up to 8 % at 530 °C.

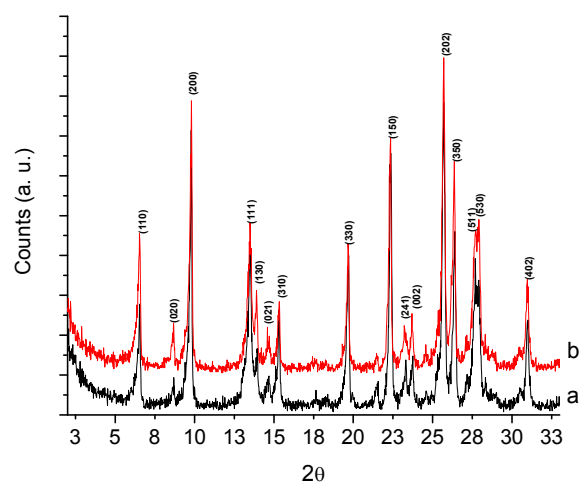


Fig. 1. Diffraction patterns of NaMor13 (a) and NiNaMor13 (b) samples before catalytic test.

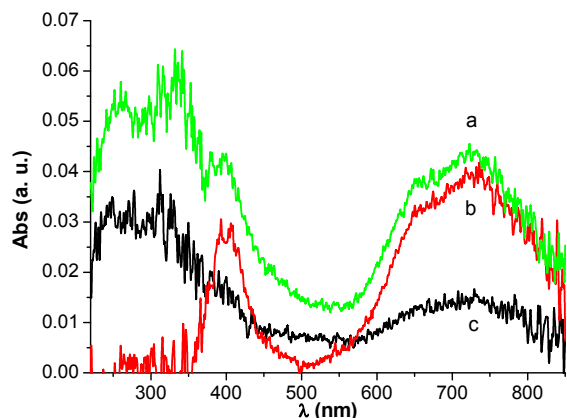


Fig. 2. Diffuse reflectance spectra of Ni/NH<sub>4</sub>Mor20 (a), Ni/NaMor13 (b) and Ni/HMor90 (c) catalysts.

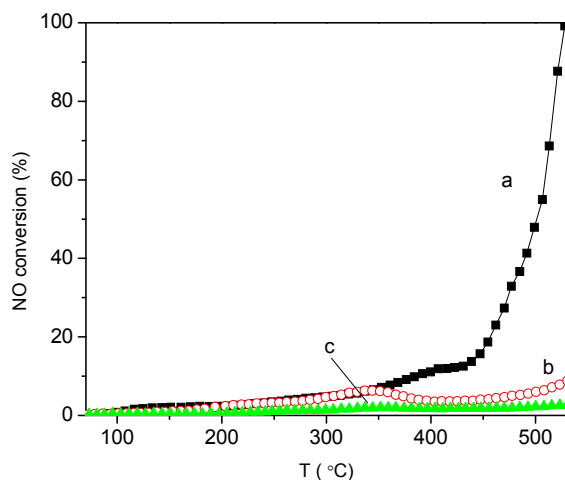


Fig. 3. NO conversion vs temperature on Ni/NaMor13 (a), Ni/NH<sub>4</sub>Mor20 (b) and Ni/HMor90 (c) catalysts.

The similar performance of NiNH<sub>4</sub>Mor20 and NiHMor90 catalysts seems to be due to partial thermal transformation of ammonium mordenite into protonic form that is carried out at temperatures higher than 350 °C.

Similar tendencies were observed by Mosqueda-Jiménez *et al.* (2003) for Ni catalysts supported on mordenite in sodium and protonic forms. They found that the catalytic activity in the SCR of NO with propene and propane was higher for the sodium form of the zeolite. The activity of samples in NO reduction with propene seems to be decreased with increasing of concentration of acid sites due to propene oligomerization and coking Vergne *et al.* (1998). The later causes blocking of active sites and pores Satsuma *et al.* (1995).

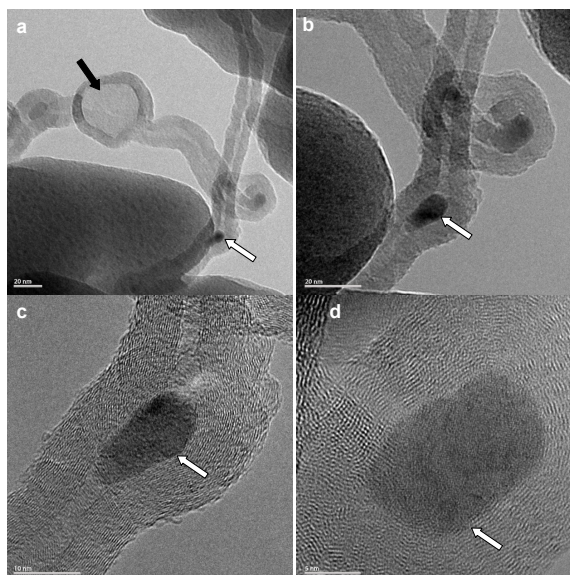


Fig. 4. TEM micrographs of the spent NiNaMor13 catalyst.

Indeed, analysis of spent catalysts by TEM reveals carbon deposit formation on the surface of NiNaMor13 catalyst (see Fig. 4). Formation of carbon nanotubes containing encapsulated nickel species (marked with white arrows) is observed. Such structures are well known to be formed during the pyrolysis of hydrocarbons over Ni metal particles Komova *et al.* (2007), Ying *et al.* (2011). The process of nanotube formation include adsorption of hydrocarbon over Ni surface, decomposition of hydrocarbon with formation of carbon atoms, their diffusion through Ni particles with final assembly of carbon nanotubes on the bottom position of nickel particles Liu *et al.* (2005). Isotropic carbon diffusion leads to partial Ni particles encapsulation MacKenzie *et al.* (2010). The shape of the carbon shows that it was formed by jumping of the metal tip at regular time intervals over similar distances (Fig. 4). This effect was explained by supposing that the metal is in a quasi-liquid state with high surface energy and poor wetting ability towards graphite carbon Li *et al.* (1999) and that the compartments on the inside of the nanotubes might be a kind of mark of the periodic condensation of graphite layers through the catalyst metal Woo Lee *et al.* (2004) (Fig. 3c). Fig. 3a shows amorphous carbon encapsulated particle (marked with black arrow), which suggests a large growth rates of carbon nanospecies Merkulov *et al.* (2005).



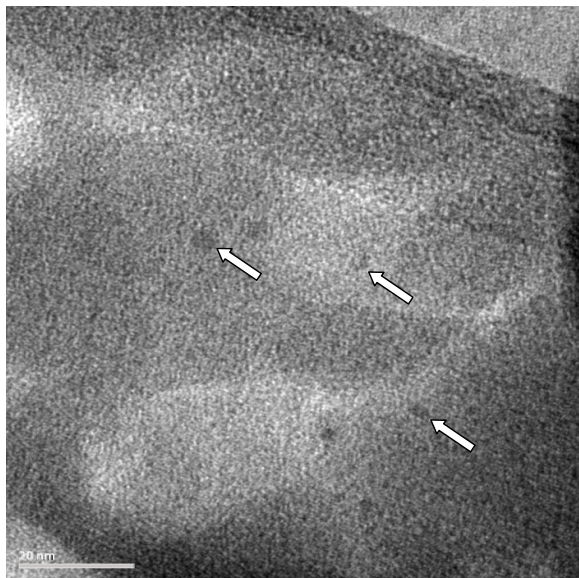


Fig. 5. TEM micrographs of the spent NiNH<sub>4</sub>Mor20 catalyst.

TEM images of NiNH<sub>4</sub>Mor20 catalyst (Fig. 5), unlike the sample NiNaMOR13, do not show formation of any carbon nanostructures. Only smaller dark Ni particles (marked with white arrows) are observed. No carbon nanostructures development is observed on the smaller Ni particles.

The results show that the high catalytic activity was found for NiNaMor13 sample only, which is also characterized with carbon nanotube formation. These two facts could be related with the nature of nickel species stabilized in mordenite framework of NiNaMor13 catalyst. The decrease of SiO<sub>2</sub>/Al<sub>2</sub>O<sub>3</sub> ratio leads to the increase of amount of exchangeable sites (Al-O-(Si-O)<sub>N</sub>-Al, with  $N \leq 3$ ), that is reflected in the increase of Ni exchanged in a NaMor13 sample. However, not only amount of nickel but the strength of Ni interaction with the silica-alumina structure depends on the arrangement of Al-centered tetrahedra in framework Bogdanchikova *et al* (2000).

Only NiNaMor13 sample is characterized with the presence of Ni species weakly bonded with zeolite framework according to the UV-Vis spectra. The easiness of red-ox transformations of Ni species is directly related with catalytic activity in de-NO<sub>x</sub> process, as it was shown by Garbowski *et al.* (1983). In contrary with NiNaMor13 catalyst other two samples manifest strong metal-support interaction by appearance of the charge transfer absorption band in UV-Vis spectra (Fig. 2). Strong interaction with zeolite matrix leads to the difficulties in red-ox

transformation of nickel species and as a consequence to the decrease of the activity in NO reduction.

On the other hand, easiness of red-ox transformation of Ni species can provoke easy formation of Ni metal particles in the presence of such reducing agents as CO and propene in the reaction mixture, which is crucial for the formation and growth of carbon nanotubes Li *et al.* (1999), Height *et al.* (2005), Liu *et al.* (2005), MacKenzie *et al* (2010). Both propene and CO could be considered as precursors for carbon nanotube formation.

For the samples characterized with high strength of Ni-mordenite interaction the formation of carbon nanotubes is not observed. Fig. 5 demonstrates only small Ni particles on the surface of NiNH<sub>4</sub>Mor20, without any detectable carbon nanostructures.

On the other hand, formed carbon nanotubes could act as active centers, thus allowing the NO reduction to continue at high temperatures Serp *et al.* (2003). As can be seen from the TEM images (Fig. 4), carbon nanostructures are characterized with a presence of structural defects on their external walls. These defects can serve both as centers for adsorption of reaction mixture components and as reducing reactant. Note that sharp increase in catalytic activity of NiNaMor13 sample begins at the high temperature, characteristic for carbon nanotubes formation over Ni metal particles due to pyrolysis of hydrocarbons Esconjauregui *et al.* (2009).

## Conclusions

It was shown that SiO<sub>2</sub>/Al<sub>2</sub>O<sub>3</sub> molar ratio is important parameter influencing the interaction of Ni species with mordenite framework. Ni species formed on mordenite NiNaMor13 with low molar ratio are characterized with low strengths of metal-support interaction, as a consequence high catalytic activity in NO reduction. In the same time easy red-ox transformation of such a species results in the formation of carbon nanostructures, those can be responsible for catalytic activity improvement as well.

## Acknowledgements

The authors acknowledge E. Aparicio, I. Gradilla, J. Peralta, V. Gradilla and E. Flores for technical assistance. This research was supported by PAPIIT IN207511, PAPIIT IN110608, PAPIIT IN224510 and CONACYT 102907 grants.

## References

- Abu-Zied, B.M., Schwieger, W. and Unger A. (2008). Nitrous oxide decomposition over transition metal exchanged ZSM-5 zeolites prepared by the solid-state ion-exchange method. *Applied Catalysis B-Environmental* 84, 277-288.
- Baerlocher, Ch., McCusker, L.B. and Olson D.H. (2007). *Atlas of zeolite framework types*, 6<sup>th</sup> edition, Amsterdam: Elsevier. v
- Bogdanchikova, N., Petranovskii, V., Machorro Mejia, R., Sugi, Y., Soto, V.M. and Fuentes, S. (1999). Stability of silver clusters in mordenites with different SiO<sub>2</sub>/Al<sub>2</sub>O<sub>3</sub> molar ratio. *Applied Surface Science* 150, 58-64.
- Bogdanchikova, N., Petranovskii, V., Fuentes, S., Paukshtis, E., Sugi, Y. and Licea-Claverie, A. (2000). Role of mordenite acid properties in silver cluster stabilization. *Materials Science and Engineering A* 276, 236-242.
- Esconjauregui, S., Whelan, C.M. and Maex, K. (2009). The reasons why metals catalyze the nucleation and growth of carbon nanotubes and other carbon nanomorphologies. *Carbon* 47, 659-669.
- Gurin, V.S., Petranovskii, V.P. and Bogdanchikova, N.E. (2002). Metal clusters and nanoparticles assembled in zeolites: an example of stable materials with controllable particle size. *Materials Science and Engineering C* 19, 327-331.
- Gurin, V., Petranovskii, V., Hernandez, M.-A., Bogdanchikova, N. and Alexeenko, A.A. (2005). Silver and copper clusters and small particles stabilized within nanoporous silicate-based materials. *Materials Science and Engineering A* 391, 71-76.
- Height, M.J., Howard, J.B., Tester, J.W. and Vander Sande, J.B. (2005). Carbon nanotube formation and growth via particle-particle interaction. *The Journal of Physical Chemistry B* 109, 12337-12346.
- Hu, Y., Griffiths, K. and Norton, P.R. (2009). Surface science studies of selective catalytic reduction of NO: Progress in the last ten years. *Surface Science* 603, 1740-1750.
- Johnson T.V. (2009). Review of diesel emissions and control. *International Journal of Engine Research* 10, 275-285.
- Komova, O.V., Simakov, A.V., Kovalenko, G.A., Rudina, N.A., Chuenko, T.V. and Kulikovskaya, N.A. (2007). Formation of a nickel catalyst on the surface of aluminosilicate supports for the synthesis of catalytic fibrous carbon. *Kinetics and Catalysis* 48, 803-811.
- Lever, A.B.P. (1984). *Inorganic electronic spectroscopy*, 2<sup>nd</sup> edition, Elsevier, Amsterdam - New York.
- Li, Y., Chen, J., Ma, Y., Zhao, J., Qin, Y. and Chang, L. (1999). Formation of bamboo-like nanocarbon and evidence for the quasi-liquid state of nanosized metal particles at moderate temperatures. *Chemical Communications* 12, 1141-1142.
- Liu, H., Cheng, G., Zheng, R. and Zhao, Y. (2005). Controlled growth of Ni particles on carbon nanotubes for fabrication of carbon nanotubes. *Journal of Molecular Catalysis A: Chemical* 225, 233-237.
- MacKenzie, K.J., Dunens, O.M. and Harris, A.T. (2010). An updated review of synthesis parameters and growth mechanisms for carbon nanotubes in fluidized beds. *Industrial and Engineering Chemistry Research* 49, 5323-5338.
- Martinez, C. and Corma, A. (2011). Inorganic molecular sieves: Preparation, modification and industrial application in catalytic processes. *Coordination Chemistry Reviews* 255, 1558-1580.
- Merkulov, I.A., Meleshko, A.V., Wells, J.C., Cui, H., Merkulov, V.I., Simpson, M.L. and Lowndes, D.H. (2005). Two growth modes of graphitic carbon nanofibers with herring-bone structure. *Physical Review B* 72, 045409.
- Mosqueda-Jiménez, B.I., Jentys, A., Seshan, K. and Lercher, J.A. (2003). Reduction of nitric oxide by propene and propane on Ni-exchanged mordenite. *Applied Catalysis B: Environmental* 43, 105-115.
- Parvulescu V.I., Grange P. and Delmon B. (1998). Catalytic removal of NO. *Catalysis Today* 46, 233-316.

- Rebrov, E.V., Simakov, A.V., Sazonova, N.N. and Stoyanov, E.S. (1999). Dinitrogen formation over low-exchanged Cu-ZSM-5 in the selective reduction of NO by propane. *Catalysis Letters* 58, 107-118.
- Rebrov, E.V., Simakov, A.V., Sazonova, N.N. and Stoyanov, E.S. (2000). Rate-determining stage in NO SCR with propane on low-exchanged Cu-ZSM-5 catalyst. *Catalysis Letters* 64, 129-134.
- Satsuma, A., Yamada, K., Mori, T., Niwa, M., Hattori, T. and Murakami, Y. (1995). Dependence of selective reduction of NO with C<sub>3</sub>H<sub>6</sub> on acid properties of ion-exchanged zeolites. *Catalysis Letters* 31, 367-375.
- Sazonova, N.N., Komova, O.V., Rebrov, E.V., Simakov, A.V., Kulikovskaya, N.A., Rogov, V.A., Olikhov, R.V. and Barannik, G.V. (1997). Catalytic and adsorptive properties of Cu-ZSM-5 catalyst synthesized by solid phase method. *Reaction Kinetics and Catalysis Letters* 60, 313-321.
- Serp, P., Corrias, M. and Kalck P. (2003). Review. Carbon nanotubes and nanofibers in catalysis. *Applied Catalysis A: General* 253, 337-358.
- Vergne, S., Berreghis, A., Tantet, J., Canaff, C., Magnoux, P., Guisnet, M., Davias, N. and Noirot, R. (1998). Reduction of NO by propene over a Cu-MFI catalyst. Investigation of the mechanism from the composition of compounds trapped in the zeolite pores. *Applied Catalysis B: Environmental* 18, 37-50.
- Woo Lee, G., Jurng, J. and Hwang, J. (2004). Formation of Ni-catalyzed multiwalled carbon nanotubes and nanofibers on a substrate using an ethylene inverse diffusion flame. *Combustion and Flame* 139, 167-175.
- Yahiro H. and Iwamoto M. (2001). Copper ion-exchanged zeolite catalysts in de-NO(x) reaction. *Applied Catalysis A-General* 222, 163-181.
- Ying, L.S., Salleh, M.A. B., Yusoff, H.B. M., Rashid, S.B. A. and Abd Razak, J.B. (2011). Continuous production of carbon nanotubes - A review. *Journal of Industrial and Engineering Chemistry* 17, 367-376.